2025-01-8784 Published 01 Apr 2025

Design and Evaluation of a Conceptual Zero-Emission Truck Model Considering Aerodynamic Efficiency

Faegheh Ghorbanishohrat, Brian McAuliffe, and Harrison O'Reilly National Research Council Canada

Citation: Ghorbanishohrat, F., McAuliffe, B., and O'Reilly, H., "Design and Evaluation of a Conceptual Zero-Emission Truck Model Considering Aerodynamic Efficiency," SAE Technical Paper 2025-01-8784, 2025, doi:10.4271/2025-01-8784.

Received: 15 Oct 2024 Revised: 08 Jan 2025 Accepted: 21 Jan 2025

Abstract

Emerging zero-emission-powertrain concepts are providing opportunities to re-shape heavy trucks for improved aerodynamic performance. To investigate the potential for energy savings through aerodynamic improvements, with a goal to inform operators and regulators of such benefits, a multi-phase project was initiated to design and evaluate aerodynamic improvements for Class 8 tractor-trailer combinations. While the focus was battery-electric and hydrogen-fuel-cell powered trucks, improvements for internal-combustion powered trucks were also examined. Previously-reported activities included a scaled-model wind-tunnel test that demonstrated the potential for up to 9% drag reduction from simple shape adaptations, with a follow-up CFD study providing guidance towards further optimization.

This paper presents wind-tunnel-test results using a high-fidelity 30%-scale model of a new aerodynamic tractor concept, with comparison to a conventional North American Class 8 tractor with a modern aerodynamic package and identical wheelbase. The study included testing of the new tractor concept along with individual parts such as air dams, under-body panels, grill/cooling-flow configurations, mirrors, wheel fairings, cab extenders, etc. The battery-electric variant of the new tractor provided a 16% drag reduction compared to the conventional truck model when using the same trailer configuration. When paired with a low-drag-trailer concept, the new tractor-trailer combination demonstrated up to 41% drag reduction compared to the conventional tractor with a standard box-van trailer. This configuration is shown to be nearly insensitive to crosswinds with a wind-averaged drag coefficient of 0.34. Examining additional cooling-flow configurations necessary for hydrogen-fuel-cell trucks showed up to 3% increase in drag associated with the extra cooling drag. Additionally, the new tractor-shaping concept applied to a conventional internal-combustion-powertrain arrangement generated 8% drag reduction compared to the conventional tractor.

Introduction

As zero-emission heavy-duty vehicles (ZEHDVs) such as battery-electric and hydrogen-fuel-cell vehicles emerge, new opportunities for improved aerodynamic performance arise due to evolving drivetrain configurations and different cooling strategies. Unlike conventional heavy-duty vehicles, ZEHDVs can adopt more streamlined shapes with advanced aerodynamic strategies. Examples of conceptual designs with conventional diesel and emerging zero-emission powertrains include prototype and production concepts like the Nikola One/Two concepts, the Shell Starship 3.0, the MAN Concept S, the Tesla Semi, and the SuperTruck 2 concepts by Volvo and Kenworth. These designs enhance energy efficiency and extend range, critical for long-haul freight. Some have provided commercial information regarding their design and fuel consumption, and some have already been introduced to the market. However, from a research perspective, the authors were unable to find credible scientific data for these newly released models to compare with this study. Understanding these aerodynamic improvements is vital for guiding energy efficiency and regulatory efforts towards decarbonizing the transportation sector.

A multi-phase project was launched to examine the aerodynamic efficiency of ZEHDVs by examining improved cab shaping for both battery-electric and hydrogen-fuel-cell configurations. In the previous phases of the project, preliminary tests at 30% scale were conducted in the 9 m Wind Tunnel using a day-cab tractor-trailer model, which was modified in terms of windscreen shape and angle, corner radii, and cooling flow rate to represent emerging zero-emission (ZE) cabs based on aerodynamic considerations [1]. The results indicated a 7-9% reduction in drag. Cab-shape optimization progressed through a parametric geometry study using computational fluid dynamics (CFD) simulations, demonstrating 8% variation in aerodynamic drag over the range of geometric changes evaluated [2]. The geometry was optimized for front face area, corner radii, windshield angle, roof angle, roof radius, bumper

© 2025 National Research Council Canada; Published by SAE International. This Open Access article is published under the terms of the Creative Commons Attribution License (http://creativecommons.org/licenses/by/4.0/), which permits distribution, and reproduction in any medium, provided that the original author(s) and the source are credited.

radius, wheel wells, and the inclusion of air dams. A 30% scaled model, guided by the CFD case studies, was designed and 3D-printed for further study via wind tunnel testing.

This paper documents a study to investigate the aerodynamic performance of the newly-designed ZE model (from the previous phases of the project) for three powertrain configurations (internal-combustion, battery-electric, and hydrogen-fuel-cell) along with various tractor and trailer aerodynamic devices. Notably, the wheelbase of the ZE cab matched the 6x4-drivetrain chassis used for a conventional sleeper-cab model, allowing the new shape to fit over the existing wind-tunnel-model chassis.

Experimental Setup

Wind Tunnel

All tests for this study were conducted in the 9 m Wind Tunnel, which is a horizontal closed-circuit wind tunnel with a square test section of 82 m^2 cross-sectional area and a length of 22.9 m.

The fan is powered by an air-cooled 6.7 MW DC motor, providing wind speeds of up to 55 m/s in an empty test section. To simulate the relative vehicle motion on the road, the NRC Ground Effect Simulation System (GESS) was used, which includes a 5.6 m-long moving ground plane and a boundary layer control system with two suction plena. The rolling road of the GESS is enclosed in the 6.1 m diameter turntable. The six components of aerodynamic forces and moments were measured using an external mechanical pyramidal balance located beneath the turntable floor. The 30%-scale models were mounted over the rolling road using streamlined struts. These struts connected the tractor-trailer models to the six-axis balance via a small opening in the turntable. Strut-tare and strut-interference corrections were quantified and applied for all tractor-trailer configurations tested in this study. The NRC Road Turbulence System (RTS) [3] was used, which creates a turbulence intensity of 4% and a turbulence length scale greater than 0.3 m (1.0 m full scale), representative of on-road turbulence characteristics experienced by road vehicles [4, 5].

Based on the speed limitations of the moving ground plane, the wind speed is 50 m/s for this study, corresponding to a Mach number of about 0.15 and a model-width-based Reynolds number of about 2.6 million. Figure 1 shows the test section configuration for this study. Testing was conducted in accordance with SAE best practices [6] and adaptations thereof specific to the NRC setup. For this testing, a floor-mounted enclosure was present at the inlet of the test section (marked as traverse assembly in Figure 1), necessary for a traffic-wake simulation system not in use for these tests. The presence of the faired enclosure was verified to not influence adversely the flow quality at the leading edge of the turntable.

FIGURE 1 Upwind view of the test section with 30%-scale HDV model with conventional sleeper-cab tractor.

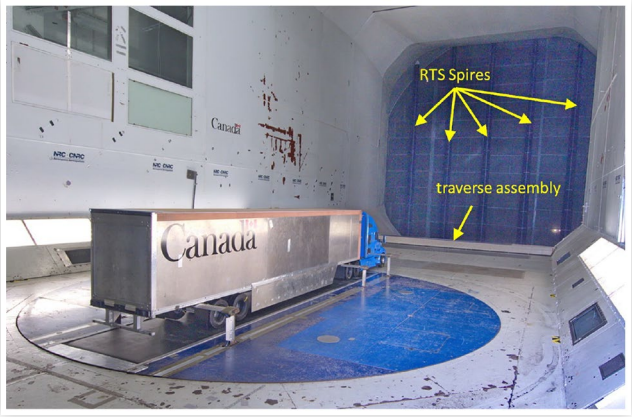

© National Research Council Canada

FIGURE 2 Tractor-trailer models: conventional sleeper-cab tractor (top), zero-emission tractor (bottom).

© National Research Council Canada

Test Models

Testing was conducted using the NRC 30%-scale tractor-trailer model. This is a detailed wind-tunnel model of a heavy-duty vehicle (HDV) designed to accommodate different cab styles and trailer types typical of HDVs on North American roads. The tractor-model chassis features an engine bay with a representative static engine model and its auxiliary components. It uses porous screens to simulate the cooling system, with vane anemometers mounted behind the front grill to measure the cooling flow rates. Two variants of the tractor model were tested in the current study. Both variants have a 6x4 axle arrangement and a tractor-trailer gap of 0.343 m (1.14 m full scale). The conventional long-sleeper-cab model, shown in the upper photograph of Figure 2 is described in detail in a previous study [7].

FIGURE 3 Under body details of the conventional sleeper-cab tractor (left) and the zero-emission tractor (right) models.

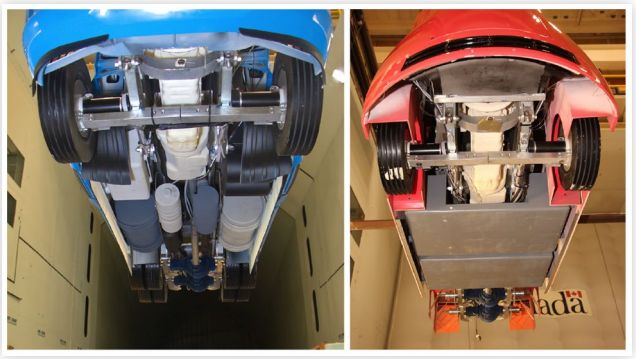

© National Research Council Canada

FIGURE 4 Zero Emission CAD model.

© National Research Council Canada

The new zero-emission cab model, shown in the lower photograph of Figure 2, was designed and developed by NRC with a focus on optimizing aerodynamics similar to characteristics found on emerging zero-emission HDV (ZEHDV) shapes. The underbody structure was adapted to accommodate simulated battery packages instead of fuel tanks. The same engine-bay, static-engine, and cooling-package models were used, but multiple cooling-airflow and underbody-panel configurations were used to represent different powertrain configurations, described in a later section. The open-underbody configurations of both tractor variants are shown in Figure 3.

The 30%-scale trailer model represents a 53-ft box van modelled after a combination of trailers on the market. It is set to a dry-van trailer configuration in this study, with the bogie positioned 0.91 m from the trailers rear surface. Details of on-road trailers incorporated into the model design include landing gear, underbody ribs, a rear-impact guard, a header and rain gutter at the top aft edge, with lights and door hardware. Figure 2 shows the standard trailer model, with standard skirt (ZE tractor) and without any drag-reduction technologies (sleeper cab tractor).

The tractors and trailer are equipped with electric-wheel-drive systems and treaded-wheels. The wheel speed matches the rolling-road speed, both of which are synchronized to the blockage-corrected wind speed of the test condition. The torque required to sustain wheel speed during testing is quantified, tared for bearing losses, and used to determine the ventilation-drag coefficient (related to torque-induced drag), which is then combined with the balance-inferred drag coefficient [8]. Although not explicitly quantified in this paper, the ventilation drag accounts for about 3-5% of the published drag-coefficient values.

ZEHDV Model Design and Development

As described in the introduction, the development of the new zero-emission tractor model was initiated with a previously-reported preliminary 30%-scale wind-tunnel test campaign using an adapted version of a day-cab tractor model [1], followed by a shape-optimization study using CFD.

A parametric CAD model was created using SolidWorks software. Vehicle geometry parameters, such as cab frontal area, height, corner and roof radii, stagnation region area, windshield and roof angles, wheelhouse shape, bumper shape, and underbody airflow, which all affect aerodynamic performance [9, 10, 11, 12, 13], were considered in defining the design parameters. An optimized cab was achieved through a parametric analysis by examining the drag changes of various individual and combined design parameters via CFD using the Ansys-Fluent software package. A 5% reduction in aerodynamic drag was identified, over the initially-selected zero-emission shape, using this approach [2].

The final geometry, shown in Figure 4, was a modified version of the CFD-selected shape, adapted to fit the chassis of the 30%-scale wind-tunnel model. These modifications resulted in an estimated increase in drag of 1% from the parametric CFD analysis design. The selected shape was reinforced for manufacturing, and a 30%-scale modular model with exchangeable parts, including cameras, mirrors, cooling ducts, air dams, grills, wheel fairings, cab extensions, underbody panels, and fan exhausts, was manufactured using an SLS (selective laser sintering) 3D printing approach. 3D-printed surfaces were mounted on a structural frame built using extruded aluminum. This frame mounted to the 30%-scale chassis as one unit to facilitate the process of switching between the new ZEHDV and the conventional truck model during testing.

To create realistic models representing various powertrain configurations, modular underbody components, grill openings, and cooling air paths were designed. The original conventional 30%-scale model included components exposed in the underbody such as the engine, fuel tanks, diesel exhaust fluid (DEF) tank, and other accessories. To adapt the model for battery-electric and hydrogen-fuel-cell powertrains, battery boxes were designed and built to replace the conventional fuel/DEF tanks and exhaust components. Additionally, a smooth underbody panel was designed and manufactured to cover all battery boxes and internal components.

FIGURE 5 Porous mudflaps used for the test model.

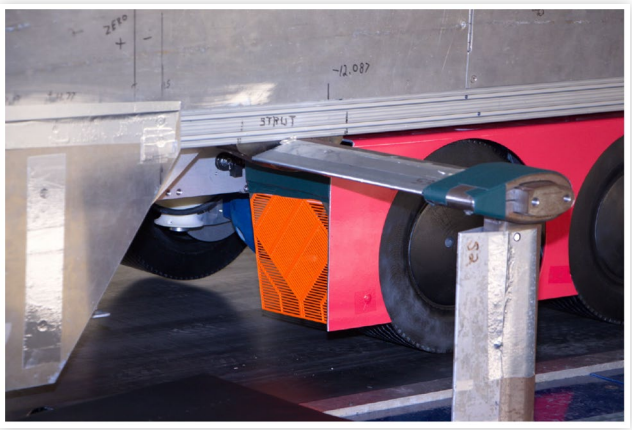

© National Research Council Canada

Solid panels were built as grill replacements to adapt the inlet cooling-air split for conventional and electric-powered HDVs, and more-porous "radiator" screen inserts were used to increase inlet cooling-flow rates for the hydrogen-fuel-cell configuration, which requires more cooling flow than conventional diesel-powered. A set of secondary cooling-flow paths were also designed within the roof-fairing assembly with top and/or side inlets and a duct exhausting into the tractor-trailer-gap region. Natural pressure gradients between the top/sides to the gap region were insufficient to induce the requisite flow rates, and could even induce reverse flow, therefore a fan was installed in the duct to force the desired flow rates. The reduced radiator porosity and the fan system were designed to double the flow rate through the tractor model. The additional cooling ducts were exposed through removal of solid cover panels. Vane anemometers installed behind the front grill and inside the inlet ducts were used to estimate flow rates and to quantify changes to the cooling airflow rates.

Interchangeable Tractor Parts

Interchangeable parts used to achieve a range of potential configurations for testing on the zero-emission-tractor model include:

- Porous Mudflaps (Figure 5): These mudflaps were designed to replicate porosity and channel-shape characteristics of available products on the market. Reynolds-number-scaling was used to define the porous-channel shapes (width and depth) rather than direct geometric scaling, to replicate the appropriate pressure-loss coefficient across the flaps. Since the wind tunnel tractor-trailer operates at approximately 50-60% of the full-scale on-road Reynolds number, the mudflap was scaled to about 50% of the slot geometries found in the market, instead of the 30%-scale that would be defined by geometric scaling.
- Under-Body Panel and Air-Dams Components (Figure 6): Under-body smoothing is a well-known feature in vehicles design to reduce aerodynamic drag, by preventing air from impacting the exposed components of the drivetrain. A smooth under-body panel was designed as a removable part for the ZE truck model. Various combinations of wheel air dams with two heights (2.5 cm and 5 cm, model scale) and with multiple widths were tested, to study their performance to deflect the air around the wheels. The influence of the combination of the under-body panel and truck side fairing can result in a drag area reduction of up to 3-4% [14].
- Mirrors and Cameras: Mirrors are essential components for safe driving; however, advancing technology offers the opportunity to replace traditional HDV mirrors with cameras. Currently, removing mirrors and replacing them with cameras is not yet legal in Canada or in the United States.

FIGURE 6 Adjustable under-body-panel and air-dam configurations.

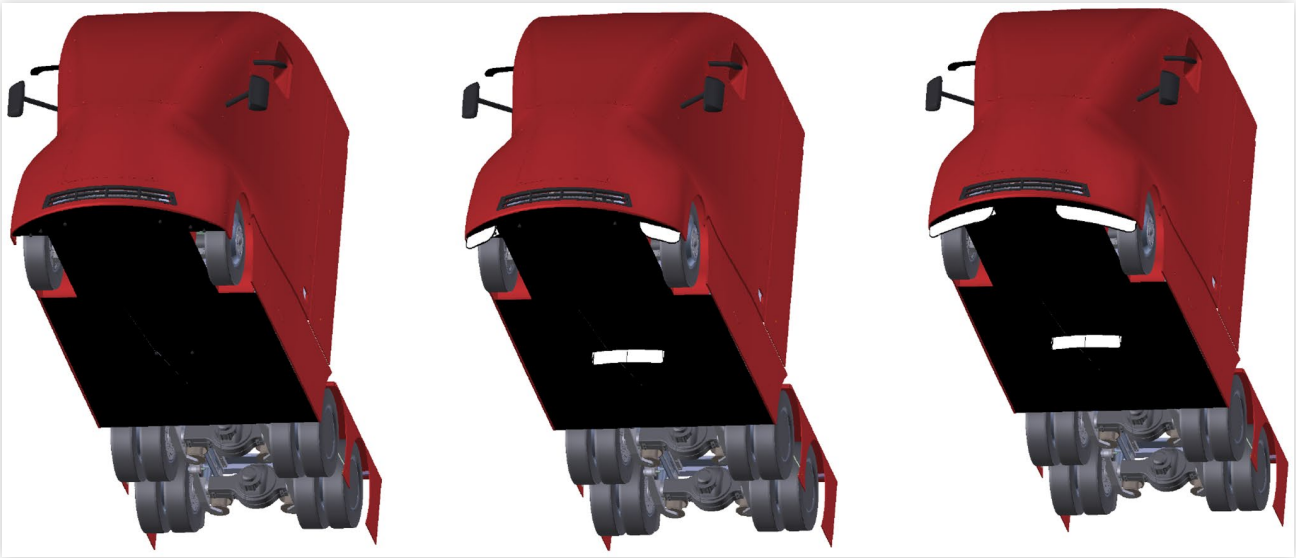

© National Research Council Canada

This study examines the effects of replacing mirrors with cameras and partially examines the impact of camera placement on the aerodynamic performance of a new HDV concept design. The mirrors and camera-enclosure models are shown on the CAD model in Figure 4. Eliminating mirrors has been reported to provide up to a 6% benefit [15]. The previously-reported preliminary experimental tests from this project showed that removing fender mirrors resulted in a 1-2% reduction in drag, while main mirrors resulted in a 3% reduction [1]. For the new ZE model, replaceable main mirrors with cameras or with blanks to eliminate them completely were designed. Additionally, two locations were defined for the cameras to study the effect of their placement on aerodynamic efficiency.

- Wheels, Drive-Wheel Fairing and Wheel Covers: Airflow around rotating wheels has complex characteristics, and preventing air from entering the wheelhouse improves aerodynamic efficiency. Wheel fairings are typically paired with wheel covers for enhanced performance, and their benefits have been reported to range from 1.5% to 2% for HDVs [15]. The NRC 30%-scale model allows for the replacement of wheels pairs with single-wide wheels and enables the addition or removal of drive wheel fairings, which have been used to evaluate the influence of these devices on aerodynamic efficiency.
- Cab Extender: The cab extender is designed with adjustable side and top panels (shown in Figure 7), providing deflections of the panels up to 5° inward and 10° outward, and with two lengths: a standard length (0.20 m model scale, 0.68 m full scale) and an extended length (0.33 m model scale, 1.10 m full scale). When studying the cab extender, it is crucial to consider crosswind conditions, as these reflect realistic on-road scenarios. Roof and cab extenders have been reported to provide about a 1-2% improvement in drag [15].

FIGURE 7 Cab extender with adjustable top and side panels, and axial fan for the roof-duct cooling flows.

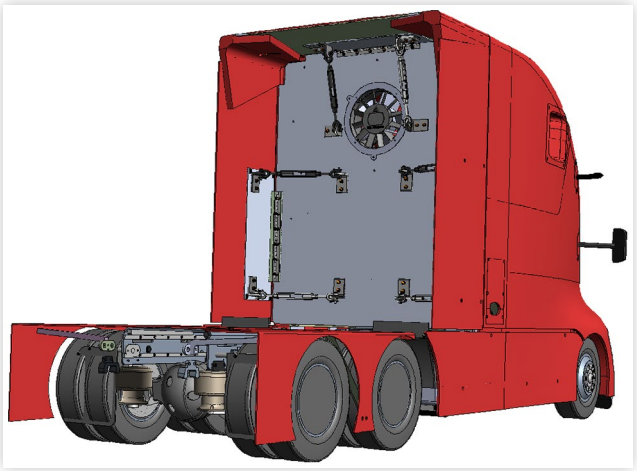

© National Research Council Canada

FIGURE 8 Adjustable front grill, with roof cooling-flow ducts open.

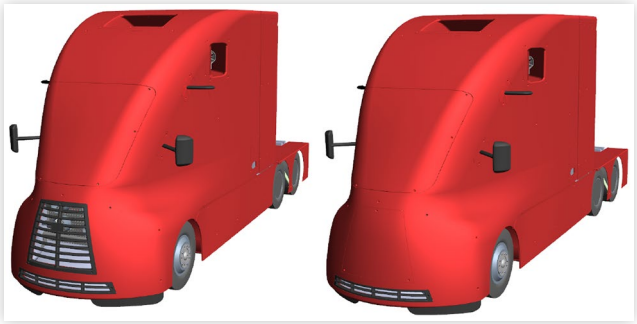

© National Research Council Canada

FIGURE 9 Annular diffuser installed over the fan exhaust for the roof-duct cooling flows.

© National Research Council Canada

- Front Grills and Cooling System: Two cooling-airflow passages have been 3D-printed with the new ZE tractor model, each with an interchangeable opening (grill or solid insert, see Figure 8), and each exhausting through the porous-screen-radiator model inside the engine bay. The radiator has interchangeable screens with different porosities. Additionally, as noted in the previous section, a secondary cooling-airflow system was designed for the hydrogen-fuel-cell configuration with ducts through the roof fairing, with both sets of ducts shown open in Figure 8. Two exhaust configurations were used for the roof ducts, with either the fan exhausting directly in the gap region (shown in Figure 7), or an annular diffuser used to diffuse the jet (shown in Figure 9).

Interchangeable Trailer Parts

Several trailer-aerodynamic devices were used in this tests, including:

- Standard Trailer Skirt: This is a front-edge-tapered skirt designed by NRC for 30%-scale tests, with a length of 2.4 m (8.0 m full scale) and a height of

FIGURE 10 Low-drag trailer model with side-skirts, large boat-tail, trailer fairing, and single-wide tires with wheel covers.

© National Research Council Canada

0.27 m (0.91 m full scale). The leading edge approximately aligns with the landing gear, and the trailing edge is just forward of the bogie wheels [16]. This skirt model is shown installed on the truck models in Figures 1 and 2.

- Extended Skirt: Shown in Figure 10, this is a combination of the standard skirt and an extended panel to cover the trailer bogie [16].
- Boat Tail: A large boat tail was designed and used by NRC for previous tests, shown installed on the trailer in Figure 10. It is a trailer base device featuring a four-panel design with all panels extending 0.37 m (1.22 m full scale) from the trailer base with a 13° inset angle.
- Front Fairing: The front fairing is mounted on front face of the trailer to reduce the trailer-tractor gap size [17]. The fairing was only used in combination with a long tractor gap extender that covers most of the gap, and is therefore not anticipated to have an influence to the test results.
- Low-Drag Trailer Roof: The low-drag trailer roof, shown in Figure 10, was designed and used in previous tests using this trailer model [17]. In this configuration, the sharp edges of the dry van trailer were rounded using a 2:1 elliptical shape on the side and front edges, within a height of 4.6 cm (0.15 m full scale). The roof is tapered downward by 4.6 cm over a distance of 0.91 m toward the rear.

Data Processing and Uncertainty

To create a single representative measure of the aerodynamic-drag performance of a ground vehicle for comparing different configurations, the wind-averaged drag coefficient (C_{WAD}) is used, defined for a specified ground speed. As defined by SAE J1252 [6], the C_{WAD} is estimated using the variation of drag coefficient (C_D) with yaw angle, combined with a typical mean terrestrial wind speed. This wind speed reflects long-term averaged conditions across the United States, weighted by the annual mileage trucks cover in each state [6]. The recent Environmental Protection Agency (EPA) regulatory methods simplify this wind-averaging process by correlating the results of the SAE method at 65 mph ground speed with an averaged drag coefficient (or drag area) calculated as an average of the C_D at yaw angles of ±4.5° [18]. In the current test program, particularly for the evaluation of incremental part changes, the EPA two-yaw-angle method was used as a metric to evaluate changes in drag performance. As such, any wind-averaged-drag-coefficient values provided in this manuscript are based on this EPA two-yaw-angle method, as follows:

$$C_{WAD} = 0.5C_D\left(-4.5^\circ\right) + 0.5C_D\left(+4.5^\circ\right) \quad (1)$$

For yaw-sweep runs with a greater range of yaw angles (typically -15° to +15°), the SAE J1252-defined C_{WAD} values (not presented here) demonstrate good agreement between the two definitions, within the experimental uncertainty of $\delta C_{WAD} \approx \delta\Delta C_{WAD} \approx \pm 0.003$ [1].

Uncertainty magnitudes have been estimated for all measured and calculated parameters presented, such as the value presented in the previous paragraph. The uncertainty analysis used here is based on the procedures established in Appendix B of SAE J1252 [6], with an adaptation for calculating the uncertainty of difference values (for example ΔC_D). In the current test program, the baseline truck configurations were tested several times (up to 5 repeated tests), providing a data set to calculate the random uncertainty associated with measurement error and repeatability error. For all but the stated wind-averaged-drag coefficient values, for which the uncertainty is stated in the previous paragraph, the estimated uncertainties are provided with the data presented in this paper.

Test Results

Cab Shape and Configuration

Several phases of aerodynamic performance testing were conducted to examine the aerodynamic characteristics of the ZE tractor shape. The tests aimed to evaluate the new cab design, its powertrain variants, and individual components, comparing their aerodynamic performance to that of the conventional sleeper cab tractor, which served as the reference model. For the tractor evaluations, a dry-van trailer configuration with side skirts was used.

The overall aerodynamic improvements made to the tractor are a combination of the cab-shape change and component changes. To distinguish these two categories of changes, two sets of data are presented in Figure 11 that show the relationship between C_D and yaw angle, compared to the corresponding conventional-cab test results. Photographs of the three test models are shown in Figure 12. A summary of the drag-change findings of this study, pertinent to this and subsequent sections of this paper, are provided in Table 1.

FIGURE 11 Drag-coefficient results for the conventional sleeper-cab tractor compared to two versions of the new cab shape, all using the same skirted dry-van trailer.

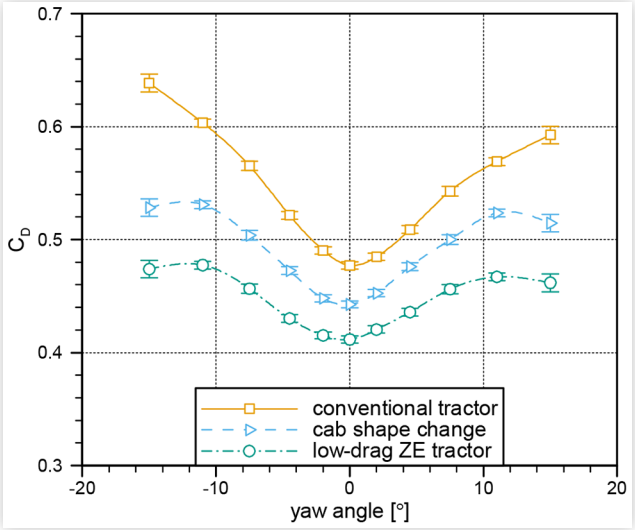

© National Research Council Canada

FIGURE 12 Conventional tractor (top), cab-shape-change tractor (middle), and battery-electric low-drag ZE tractor (bottom) test configurations associated with data in Figure 11.

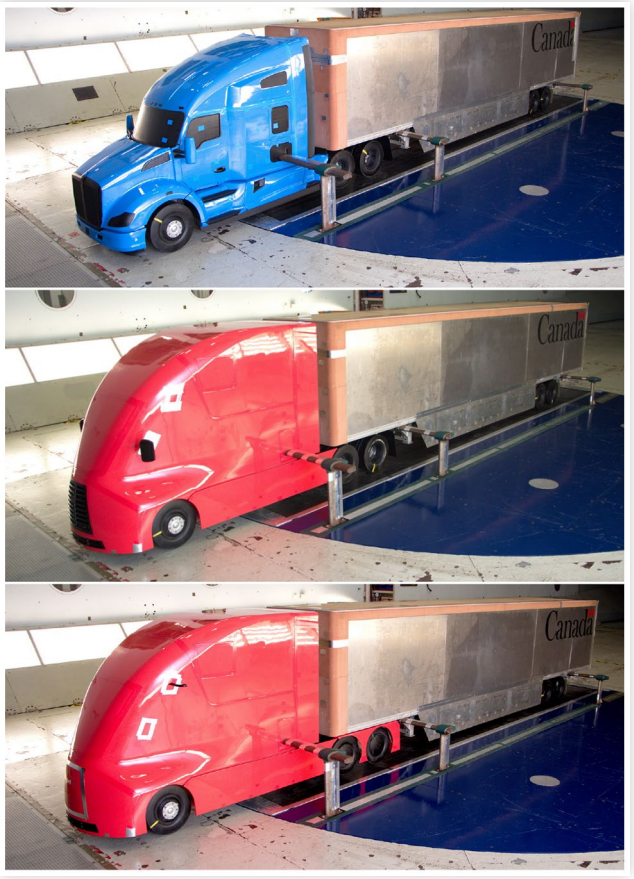

© National Research Council Canada

TABLE 1 Changes to wind-averaged-drag coefficient from component changes and combinations tested in the study. Uncertainty estimate is $\delta\Delta C_{WAD}$ = ±0.003, which is approximately 0.7%, with bold values are non-quantifiable changes.

Category	Shape or Component Change	ΔC_{WAD} ± 0.003	(±0.7%)
Tractor	Cab-shape change (relative to conventional)	-0.041	(-7.9%)
	Low-drag ZE tractor (relative to conventional)	-0.082	(-15.9%)
Drivetrain	Drive-wheel fairings	-0.009	(-2.1%)
	Single-wide wheels with covers	**-0.001**	(**-0.3%**)
Under-body	Wheel air dams	**-0.002** to **+0.002**	(**-0.4%** to **+0.4%**)
	Full-width air dams	**0.000** to +0.009	(**0%** to +2.0%)
	Long cover panel	-0.007	(-1.6%)
	Aft-centre air dam (on long cover panel)	-0.005	(-1.1%)
Visibility	Mirror removal	-0.012	(-2.7%)
	Camera addition	**+0.001** to **+0.003**	(**+0.2%** to **+0.7%**)
Cab Side Extenders	0.13 m extension (0.42 m full scale)	-0.005	(-1.2%)
Cooling Flows	Open upper grill (relative to ZE configuration)	+0.012	(+2.6%)
	Close lower grill (relative to ZE configuration)	-0.005	(-1.1%)
	Fuel-Cell variant: Increased front-grill cooling	+0.004	(+0.9%)
	Fuel-Cell variant: Top duct (no diffuser)	+0.010	(+2.3%)
	Fuel-Cell variant: Top duct (annular diffuser)	+0.004	(+1.0%)
	Fuel-Cell variant: Side ducts (annular diffuser)	+0.013	(+3.0%)
ZE Tractor and Trailer	Low-drag tractor with low-drag trailer	-0.177	(-34.4%)
	Low-drag tractor (covered lower grill) with low-drag trailer	-0.182	(-35.3%)

Changing only the cab shape while maintaining an open front grill (the same cooling flow rate) and under-body region, as would be found on a diesel-powered version of the tractor, resulted in a drag reduction of ΔC_{WAD} = 0.041 (8%). This cab shape demonstrates a greater improvement at higher cross winds, as observed at ±15° (average ΔC_{WAD} = 0.093, or 15%) for which the C_D values are lower than the values at ±11° yaw angle. This improvement under cross winds arises from the large side-corner radii that generate significant suction on the leeward side of the tractor, enhancing the thrust component of the overall drag contributions. This strong surface suction generates forward thrust in the direction of motion, as highlighted in the shape-sensitivity CFD study under previous activities of this project [2]. The new shape also demonstrates improved yaw-symmetry in the drag-coefficient data.

To represent a battery-electric "low-drag ZE tractor" configuration, the upper grill was closed with a contoured 3D-printed solid panel, mirrors were removed and camera enclosures were added, the under-body was covered with a smooth panel and an aft-centre air dam, the dual-drive-wheel assemblies were swapped for single-wide tires with wheel covers, a fairing surrounding the drive wheels was installed, and the solid mudflaps were exchanged for the Reynolds-number-scale porous mudflaps (bottom image in Figure 12). The drag-coefficient performance data for this configuration are also included in Figure 11. These changes provide the same magnitude of wind-averaged-drag reduction as the cab-shape change with ΔC_{WAD} = 0.041 (8%), with less sensitivity in the drag-reduction values with yaw angle. The overall change for the low-drag ZE tractor relative to the conventional tractor with the same skirted trailer is ΔC_{WAD} = 0.082 (16%), with maximum reduction at ±15°yaw angle of about 24%.

The following sections provide results for specific component changes made to the tractor model, leading to the large drag reductions observed between the "cab shape change" and "low-drag ZE tractor" configurations of Figure 11. A summary of the drag-change findings are provided in Table 1. All wind-averaged-drag-coefficient results stated in this and later sections have an estimated uncertainty of ±0.003.

Drive Wheels with Fairings and Covers

Wheel fairings prevent air from impinging the rotating bluff tires, and wheel covers are commonly used to prevent air entering the cavity of the wheel rim. These devices also help to guide the airflow along the body of the tractor before entering the trailer-under-body region. Wheel fairings have been reported to provide a 1.5-2% improvement in fuel economy, while no scientifically-demonstrated benefits have been observed for wheel covers installed only on tractors [15]. Single-wide tires, often named "super singles," save fuel as a result of a reduced contact patch, but have also been found to have a beneficial aerodynamic impact due to their smaller frontal area when replacing all tractor and trailer dual wheel sets [8].

The wheel fairings designed for the new ZE tractor model provide a drag reduction of ΔC_{WAD} = 0.009, about 2%. In this study, the effect of wheel covers was not examined explicitly, but they were included on the single-wide-tire models used for the low-drag ZE tractor configuration. An evaluation of the effect of drive-wheel type (traditional duals versus single wides) showed a non-measurable effect with ΔC_{WAD} = 0.001. Previous work using the same 30%-scale chassis with an older conventional sleeper-cab tractor and non-skirted dry-van trailer showed benefits of single-wide tires (ΔC_{WAD} = 0.011, about 2%) and wheel covers (ΔC_{WAD} = 0.006, about 1%) but when applied to the tractor drive axles and to the dual-axle trailer-bogie wheels [8]. The low drag reduction observed here, for just the tractor wheels, is likely due to the improved shielding resulting from the wheels fairings that limit the benefits of the single wides and covers.

Under-Body Configurations

Mitigating under-body flow rates is an effective way to reduce drag by preventing air from impinging on the wheels and the exposed under-body components. Flexible air dams extending towards the ground to shield the wheels or the under-body is a common aerodynamic strategy for tractors. The precursor CFD study showed a potential benefit from air dams, and suggested the location, the width, and the height are important geometric parameters [2].

In this experimental study, air dams were studied in combination with and without under-body panels. All air-dam tests were conducted using the wheel fairings and covers for the single-wide-tire drive-axle wheels. Regardless of location, width, height, and under-body configuration, wheel air dams did not show any quantifiable changes with all ΔC_{WAD} values in the range of ±0.002, within the uncertainty bounds of ±0.003. The CFD results suggested the tall wheel air dams would provide a benefit on the order of 2%, with drag-accumulation plots showing that increased fore-body drag was more than offset by improvements downstream due to the changes in the under-body flow at the drive-axle wheels or the trailer-bogie wheels. The inability of Reynolds-averaged Navier-Stokes (RANS) methods to predict reliably bluff-body wakes and their subsequent impingement with other components is a likely contributor to the discrepancy between the CFD and experimental results [19, 20]. This suggests that air-dam design or optimization for heavy trucks should be approached using experimental techniques (with appropriate boundary conditions) or using scale-resolving CFD approaches, rather than RANS-based CFD.

For the forward-mounted air dams, only the tall full-width air dam showed a quantifiable result, increasing wind-averaged drag by +0.009 (+2%). The discrepancies with the CFD results suggest that air-dam design or optimization for heavy trucks should be approached using

FIGURE 13 Drag-coefficient results for the ZE tractor configuration with and without an under-body panel.

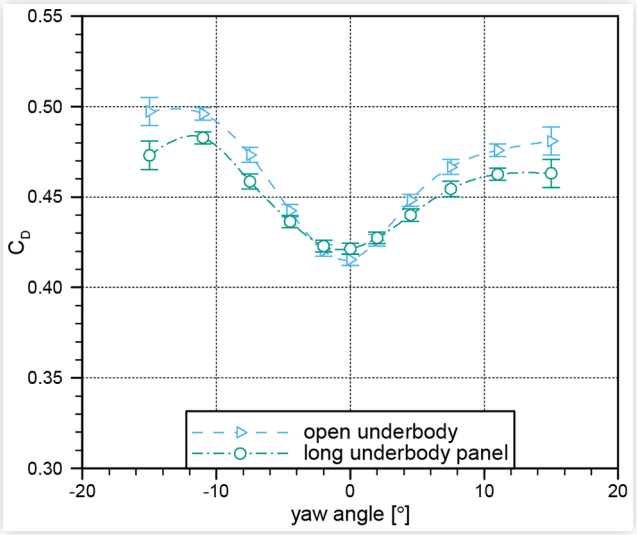

© National Research Council Canada

experimental techniques (with appropriate boundary conditions) or using scale-resolving CFD approaches, rather than RANS-based CFD.

Adding an under-body panel resulted in a reduction of wind-averaged drag (ΔC_{WAD} = -0.007, -1.6%). Figure 13 shows the drag-coefficient performance with yaw angle of two configurations of the ZE tractor model, with and without the underbody panel. There is a distinct change in benefit with yaw angle, demonstrating that covering the under-body increases the drag at 0° yaw angle, and only decreases drag for yaw-angle magnitudes of about 4.5° and larger. Pressure taps mounted to the drive-axle casings in the tractor under-body (measurements not shown here) indicated increased stagnation for 0° yaw-angle conditions with the under-body panel, suggesting the smooth under-body has less resistance to airflow and permits a greater flow rate in the under-body, which subsequently impinge on downstream components increasing the overall drag. This is a distinct example of the importance of using wind-averaged metrics to evaluate aerodynamic performance of road vehicles.

As noted above, wheel air dams did not provide a measurable change for the covered under-body configuration. The only air-dam configurations that produced beneficial results were the aft-mounted center air dams (either tall or short), with Figure 6 showing the location of the centre air dam. Both center air dams, with height variants of 2.5 cm and 5 cm (8 cm to 16 cm full scale), resulted in drag coefficient changes of about ΔC_{WAD} = -0.005 (approximately 1%), in alignment with the precursor CFD predictions. The short aft-center air dam was selected for all subsequent testing.

The combination of adding an under-body panel and an aft-center air dam resulted in a drag reduction of ΔC_{WAD} = -0.012 (approximately 2.8%) for the battery-electric ZE-tractor configuration with only the lower-front grill open. A similar magnitude of drag reduction was found for this under-body configuration applied to the internal-combustion version of the tractor with both front grills open, suggesting no measurable interactions between the cooling drag and the under-body optimization.

Mirrors and Cameras

Although not yet permitted for sole use in North America, the use of camera systems for rear visibility instead of mirrors is a suitable way to reduce drag, and are considered part of the low-drag ZE-tractor concept in this paper. Removing the camera-enclosure models or changing their locations on the ZE-tractor body, without mirrors, revealed a negligible increase in wind average drag, within the experimental uncertainty. Adding mirrors to the ZE tractor increased the wind-averaged drag by ΔC_{WAD} = +0.012 (approximately 2.7%). This is in agreement with experimental results performed in previously reported preliminary phase of this study [1].

Cab Extenders

The cab extenders for the ZE model were designed with adjustable side and top panels, with two lengths allowing for an extension between them of 0.13 m (0.42 m full scale). In the extended configuration, the panels cover most of the gap between the tractor and trailer.

The frontal profile of the ZE tractor model matched the width and height of the trailer, such that aligning the panels parallel to the sides and top of tractor and trailer structures provided the optimum flow transfer from tractor to trailer, avoiding impingement on the trailer side and top corners, and resulting in the lowest aerodynamic drag. Adjustments of panel angles were tested for yawed-flow conditions, but did not show any improvements within the 3°-angle-increment changes attempted.

The longer cab-extender panel was tested with the low-drag EV tractor configuration. Extending the panels to nearly fill the gap reduced the wind-average drag by ΔC_{WAD} = -0.005 (1.2%). This extension is not part of the low-drag-ZE-tractor configuration of Table 1, but is included when paired with the low-drag trailer discussed in a later section.

Cooling Flows

Cooling drag, associated with the diversion of flow through the body to cool the powertrain and other components, is an important contribution to the overall drag of a heavy truck. Battery-electric vehicles have the benefit of reduced cooling needs compared to the conventional diesel trucks, such that large cooling-flow inlets are not necessary at the front of the tractor. Hydrogen-fuel-cell trucks require more cooling flow than battery-electric or diesel configurations due to the low operating temperatures of the fuel-cell systems (lower temperature differentials require more cooling flow rate). The different internal-flow configurations of the ZE-tractor

model provide an opportunity to examine the impact of these cooling-flow configurations on the aerodynamic drag of these different powertrain configurations. Table 1 provides results for the change in wind-average drag for different cooling-flow changes to the ZE tractor model.

Simulating a diesel version of the tractor model, with both sets of front grills open instead of only the bottom grill, increases the wind-averaged drag by a large amount, ΔC_{WAD} = +0.012 (+2.6%). This configuration, with both grills open, has an equivalent cooling-flow rate as conventional-tractor models tested using the same chassis (average wind speed approximately 25% of the freestream wind speed), as indicated by six vane anemometers mounted forward of the simulated radiator. Covering up the lower grill, such that no cooling flow passes through the model, reduces the drag with ΔC_{WAD} = -0.005 (-1.1%).

Three methods were examined to increase the cooling flow through the model for a hydrogen-fuel-cell variant of the tractor. Any such changes in a real truck will require fans to draw-in more cooling flow, irrespective of how they were simulated in this test. The increased energy-use requirement for these fans is not considered in this analysis, only the effect on measured aerodynamic drag.

Increasing the flow rate through the front grills was accomplished by increasing the porosity of the simulated radiator. Target flow-rate increases through the model were 50% to 100%. Removing the radiator screens increased the flow rate by about 80%, as indicated by the vane anemometer speeds, which increased the wind-averaged drag of the model by ΔC_{WAD} = +0.004 (+0.9%).

Many prototype or near-production fuel-cell-powered vehicles incorporate additional cooling capacity via fans located at the base of the tractor, sometimes with no apparent consideration for the impact to aerodynamic performance of the vehicle. The two alternate cooling-flow paths embedded in the roof fairing (see Figure 8) were used as a means to examine potential impacts on aerodynamic drag of such approaches. Vane anemometers were embedded in the ducts (one in each side duct and two in the top duct) to estimate the flow rates. Exact quantification is not possible due to the spatial variability of the flow through the ducts, but it is estimated that the flow rates through the fan for the results presented here are in the target range of 50% to 100% of inlet-grill flow rates.

Results for the roof-duct-cooling study are provided in Table 1 for three configurations. Using the top duct, the drag increase associated with flow through the duct exhausting directly from the axial fan into the gap region is ΔC_{WAD} = +0.010, (+2.3%), is much greater than the case for increased front-inlet cooling. When an annular diffuser is installed (shown previously in Figure 9), the drag increment is reduced to a value on par with the front-inlet option (ΔC_{WAD} = +0.004, +1.0%). Surface-pressure data from the front face of the trailer model (data not shown here) indicate localized increased pressure from the non-diffused fan exhaust, but a negligible change with the diffuser installed, suggesting the change in the exhaust-flow patterns within the gap region have a measurable influence on the cooling drag. With side ducts open instead of the top duct, a greater drag increase was observed than any other cooling-flow configuration (ΔC_{WAD} = +0.013, +3.0%), even with the annular exhaust diffuser. The anemometer measurements from the side ducts indicate possible flow separation in or around the side duct openings, often causing asymmetric flow splits even without cross winds, suggesting improvements in the duct shapes may provide better drag performance.

The cooling-drag results presented here are based on a preliminary examination of the issue, to highlight the potential impacts of additional cooling needs in some zero-emission trucks. These results suggest there is a potential for aerodynamic optimization of cooling drag for hydrogen-fuel-cell-powered tractors.

Combination with Trailer Technologies

The ZE-tractor-development study used a skirted dry-van trailer as the basis for its performance quantification. Trailer-aerodynamic technologies provide an opportunity to further reduce the drag of the ZE-truck concept. The low-drag-ZE-tractor model, with the longer cab extenders, was paired with a low-drag trailer (shown earlier in Figure 10) that included extended side skirts, a large 4-panel boat tail, a front fairing, porous mudflaps, single-wide wheels with wheel covers, rounded roof edges along the sides and front, and a tapered aft roof. The performance of this tractor-trailer configuration is compared to conventional-tractor and other low-drag-ZE tractor configurations in Figure 14. The trailer-aerodynamic improvements with the longer cab extenders generate a significant drag-reduction improvement over the low-drag-ZE-tractor with skirted-trailer configuration (ΔC_{WAD} = -0.095, -22%). As noted in Table 1, relative to the conventional tractor with

FIGURE 14 Drag-coefficient performance for various tractor-trailer configurations tested, covering the full minimum-to-maximum range of drag coefficients observed.

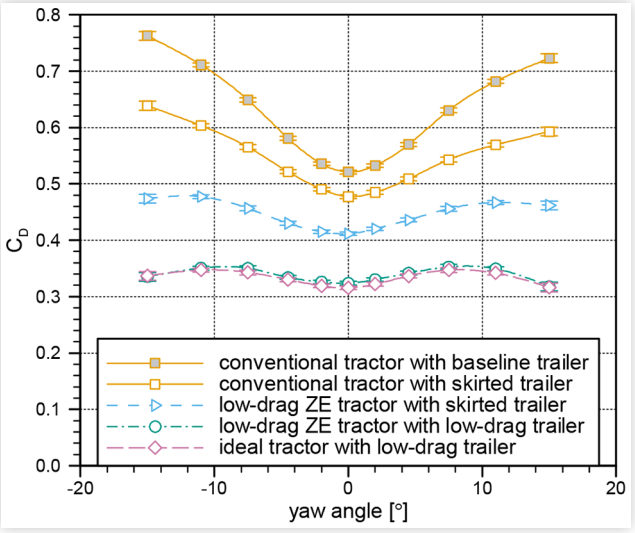

© National Research Council Canada

skirted trailer, the drag reduction is on the order of one third (ΔC_{WAD} = -0.177, -34%). When compared to the conventional tractor with standard trailer, which is still a common configuration found on the roads today, the drag reduction is even more significant (ΔC_{WAD} = -0.237, -41%). As a last attempt to reduce the drag of the tractor-trailer combination during the test program, the lower front grill was replaced with its solid smooth-surface version. Although this represents a non-practical truck with no cooling flow, an extra 1% drag reduction was observed, providing the maximum observed drag reduction for this "ideal tractor" configuration over the conventional-tractor-with-standard-trailer of ΔC_{WAD} = -0.242 (-42%).

As with the low-drag-ZE tractor, the low-drag trailer provides larger drag reductions at higher yaw angles, reducing even further the sensitivity to yaw angle. This configuration is nearly insensitive to cross winds, with drag coefficients decreasing for yaw angles greater than about ±7.5°. Salari and Ortega [12] discuss similar concepts and attribute the reduction in drag at higher yaw angles to higher front-corner suction, or enhanced thrust as mentioned earlier, and with streamlining of the aft-trailer section, such that a truck shape begins to act like a sail boat that can generate thrust and move into the wind. This relates to the orientation of the aerodynamic force vector that, despite always having a positive drag contribution in the wind-axis direction, can result in negative body-axis drag when the body is at yaw relative to the wind. Despite not achieving negative drag coefficients with this more-practical concept, the achievement of low yaw-angle-sensitivity is significant. For the low-drag-ZE with low-drag-trailer, the wind-averaged drag coefficient (C_{WAD} = 0.338) is only marginally higher, about 4%, than the 0°-yaw-angle value (C_{D0} = 0.325).

Conclusions

This paper presents an experimental study conducted at 30% scale in the NRC 9 m Wind Tunnel to investigate the aerodynamic efficiency of ZEHDVs with various powertrain configurations. For this study, an aerodynamically-optimized ZE tractor shape designed and developed through precursor CFD simulations was used. It features a modular model with exchangeable parts to investigate drag reduction via various tractor-and trailer-aerodynamic concepts and technologies. The newly-designed tractor uses the same 6x4-configured chassis as a conventional-tractor model, allowing for a direct comparison of the new cab geometry with a model representing a mid-2010's production North American Class 8 tractor. Findings of the study include:

- The testing demonstrated 8% drag reduction for a diesel-powered configuration for which only the cab shape was changed. The new shape showed significant improvement in cross-wind conditions, attributed to the large side-corner radii and their effect on frontal pressure.
- Modifying the model to represent an optimized battery-electric vehicle by closing the upper front grill, adding a smooth under-body panel with aft-center air dam, drive-wheel fairings, porous mudflaps, and switching dual-tire assemblies to single-wide-tire models with wheel covers resulted in a 16% drag reduction compared to the conventional tractor paired with the same skirted dry-van trailer.
- The effects of individual tractor-aerodynamic improvements such as mirror removal, the addition of drive-wheel fairings, and lengthening the cab extender showed similar aerodynamic-efficiency improvements as reported for conventional sleeper-cab tractors.
- Increased cooling-flow demands for hydrogen-fuel-cell-powered ZE tractors will increase the aerodynamic drag of the tractor, with different strategies for inlet and exhaust configurations examined here providing a range of wind-averaged-drag increases up to 3%.
- Pairing the optimized low-drag-ZE tractor model with a longer cab extender and a low-drag trailer achieved a 41% reduction in wind-averaged drag compared to the conventional sleeper-cab paired with a standard dry-van trailer.

The results indicate the potential for optimizing the aerodynamic performance of emerging ZE tractors, which can lead to improved fleet performance and energy savings. Although the focus of this project was to examine tractor-aerodynamic improvements, previously-devised trailer-aerodynamic improvements provided greater drag reductions, suggesting that trailers remain the low-hanging fruit for aerodynamic improvements to commercial vehicles.

Acknowledgements

This work was co-funded by Transport Canada's ecoTECHNOLOGY for Vehicles program and the National Research Council Canada's Clean and Energy Efficient Transportation program. The views and opinions of the authors expressed herein do not necessarily state or reflect those of Transport Canada. Recognition is also given to Rohit Saha of Cummins for providing insights on cooling-drag challenges for hydrogen-fuel-cell trucks.

References

1. McAuliffe, B.R., Ghorbanishohrat, F. and Barber, H. "Preliminary Investigation Towards Next Generation Truck Design for Aerodynamic Efficiency," NRC Report LTR-AL-2022-0069, 2022, doi:10.4224/40002956.
2. Ghorbanishohrat, F. and McAuliffe, B.R., "Shape Optimization Investigation of Next Generation Truck Design for Aerodynamic Efficiency," in *Proceedings of the*

FKFS Conference on Vehicle Aerodynamics and Thermal Management 2023, Stuttgart, Germany, 2023.

3. McAuliffe, B.R. and D'Auteuil, A., "A System for Simulating Road-Representative Atmospheric Turbulence for Ground Vehicles in a Large Wind Tunnel," SAE Technical Paper 2016-01-1624 (2016).
4. Smith, N.P., "Wind Gusts Measured on High-Speed Roads," MIRA Report 1972/7, The Motor Industry Research Association, 1972.
5. Wordley, S.J. and Saunders, J.W., "On-Road Turbulence: Part 2," SAE Technical Paper 2009-01-0002 (2009).
6. SAE J1252, "SAE Wind Tunnel Test Procedure for Trucks and, Uses," Surface Vehicle Recommended Practice J1252, 2012.
7. McAuliffe, B., Barber, H., and Ghorbanishohrat, F., "The Influence of Traffic Wakes on the Aerodynamic Performance of Heavy Duty Vehicles," *SAE Int. J. Adv. & Curr. Prac. in Mobility* 5, no. 6 (2023): 2193-2214, doi:https://doi.org/10.4271/2023-01-0919.
8. McAuliffe, B.R., "The Influence of Wheel and Ground Effects on the Aerodynamic Drag of a Tractor-Trailer Combination," SAE Commercial Vehicle Engineering Congress Presentation 17CVA-0019, 2017.
9. Buscariolo, F.F., Alves, J.C.L., Maruyama, F.K., Della Volpe, L.J. et al. "Truck Trailer Aerodynamic Design Optimization through CFD Simulations," in *28th SAE BRASIL International*.
10. Hariram, A., Koch, T., Mardberg, B., and Kyncl, J., "A Study in Options to Improve Aerodynamic Profile of Heavy-Duty Vehicles in Europe," *Sustainability* 11, no. 19: 5519, doi:10. 3390/su11195519.
11. Peng, J., Wang, T., Yang, T., Sun, X. et al., "Research on the Aerodynamic Characteristics of Tractor-Trailers with a Parametric Cab Design," *Applied Sciences* 8, no. 5: 791, doi:10. 3390/app8050791.
12. Salari, K. and Ortega, J., "Aerodynamic Integration Produces a Vehicle Shape with a Negative Drag Coefficient," *Proceedings of the National Academy of Sciences* 118 (2021): e2106406118, doi:10.1073/pnas.2106406118.
13. Wasik, M. and Skarka, W., "Aerodynamic Features Optimization of Front Wheels Surroundings for Energy Efficent Car."
14. "Support for Preparation of the Impact Assessment for CO2 Emissions Standards for Heavy Duty Vehicles," TNO Report TNO 2018 R10332 CLIMA.C.2./FRA/2013/0007 with ref. Ares (2016)3981250, TNO, TU Graz, CE Delft and ICCT, 2018.
15. Mihelic, R. and Mike Roeth, D.S., "Confidence Report on Tractor Aerodynamic Device Solutions," Confidence Report, North American Council for Freight Efficiency, 2020, accessed 2016, https://nacfe.org/research/technology/tractoraerodynamics.
16. McAuliffe, B.R. and Kirchhefer, A. "Improving the Aerodynamic Efficiency of Heavy Duty Vehicles: Commissioning of the Road Turbulence System and the 30% Scale Tractor-Trailer Model," NRC Report LTR-AL-2015-0274, National Research Council Canada, 2015.
17. McAuliffe, B.R., "Improving the Aerodynamic Efficiency of Heavy Duty Vehicles: Wind Tunnel Test Results of Trailer-Based Drag-Reduction Technologies," NRC Report LTRAL-2017-0272, National Research Council Canada, 2015.
18. U.S. Environmental Protection Agency and U.S. Department of Transportation, "Greenhouse Gas Emissions Standards and Fuel Efficiency Standards for Medium- and Heavy-Duty Engines and Vehicles - Phase 2," US Federal Register 81(206), 73478-74274, 2016.
19. Page, G. and Walle, A., "Towards a Standardized Assessment of Automotive Aerodynamic CFD Prediction Capability - AutoCFD 2: Windsor Body Test Case Summary," SAE Technical Paper 2022-01-0898 (2022), doi:https://doi.org/10.4271/2022-01-0898.
20. Hupertz, B., Lewington, N., Mockett, C., and Ashton, N.E.A., "Towards a Standardized Assessment of Automotive Aerodynamic CFD Prediction Capability - AutoCFD 2: Ford DrivAer Test Case Summary," SAE Technical Paper 2022-01-0886 (2022), doi::https://doi.org/10.4271/2022-01-0886.

© 2025 National Research Council Canada; Published by SAE International. This Open Access article is published under the terms of the Creative Commons Attribution License (http://creativecommons.org/licenses/by/4.0/), which permits distribution, and reproduction in any medium, provided that the original author(s) and the source are credited.

Positions and opinions advanced in this work are those of the author(s) and not necessarily those of SAE International. Responsibility for the content of the work lies solely with the author(s).

ISSN 0148-7191